

Defence Science Journal, Vol. 53, No. 4, October 2003, pp. 393-402
© 2003, DESIDOC

Underwater Explosion Damage of Ship Hull Panels

K. Ramajeyathilagam

Naval Science & Technological Laboratory, Visakhapatnam-530 027

and

C.P. Vendhan

Indian Institute of Technology Madras, Chennai-600 036

ABSTRACT

Underwater explosion is a major threat to ships and submarines in a war environment. The prediction of the mode and the extent of the failure is an essential step in designing for shock loading. The localised failure in a hull panel is severe compared to the global response of the ship. In this study, an attempt has been made to predict the response and failure modes of three types of hull panels (flat, concave, and convex). The shock loading on the hull panel has been estimated based on the Taylor's plate theory. The numerical analysis has been carried out using the CSA/GENSA (DYNA3D) code that employs nonlinear finite element model.

Keywords: Underwater explosion, failure mode, hull panel, shock loading, finite element model, deformation

1. INTRODUCTION

A ship/submarine hull consists of a variety of hull panels welded together to form the required shape and size. Underwater explosion is a major threat to the ship/submarine structures. The failure generally initiates in a hull panel. Understanding the mode and extent of damage of hull panels exposed to shock loading is the first step towards designing shock-hardened ships. The localised behaviour of hull panels to underwater explosion is quite complex involving large deformation, high strain rates, material and geometric nonlinearities and fluid-structure interaction.

Under explosive loading, three failure modes, namely, large deformation (mode I), tensile tearing

(mode II), and shear failure (mode III) have been established for clamped beams¹, and later, for plates subjected to air blast loading². "Nurick and Shave carried out further experimental studies on square plates and classified mode II as mode II* (partial tearing), mode IIa (complete tearing with increasing mid-point deflection), and mode IIb (complete tearing with decreasing mid-point deflection).

In the underwater shock area, Ahmed⁵, et al. carried out experimental studies on hull panels subjected to underwater explosion to establish the large deformation behaviour. Ramajeyathilagam⁶, et al. studied the large deformation and tensile tearing behaviour of rectangular plates subjected to underwater explosion both experimentally and numerically. In an experimental study,

Re-revised 16 August 2002

Ramajeyathilagam⁷ found that very thin plates exhibited central rupture and counter-intuitive behaviour. Large deformation behaviour of cylindrical shell panels to underwater shock were also studied by Ramajeyathilagam⁸, *et al.* based on shock tank experiments and finite element analysis. Authors have found that a nonlinear finite element model employing average strain rates for the effects of dynamic plasticity yielded deformation values that were in reasonable agreement with the shock tank test results.

The permanent deformation values of test panels (< 4 mm thickness) when plotted in a nondimensional form against yield stress showed a linear-fit. Therefore, it was thought worthwhile to investigate a real-life hull panel using the finite element analysis, so as to bring out its behaviour under shock loading. For this purpose, three types of shallow hull panels (concave, convex, and flat) used in typical ship structures have been considered. The concave and the convex hull panels have been assumed to have a shell rise ratio of 0.05. The numerical study carried out on hull panels with projected dimensions 1.50 m × 0.60 m × 0.012 m (thick) using⁹ the CSA/GENSA (DYNA3D) finite element code has been presented. A brief description of the empirical form of shock pressure loading considered in conjunction with the Taylor's plate theory has been given. Also, an outline of the finite element model employed and the failure criterion have been presented and the numerical results on typical hull panels discussed.

2. SHOCK PRESSURE LOADING

The explosion energy produced is a function of the charge weight and the stand-off distance. The empirical pressure-time history at any location with an instantaneous pressure increases, followed by a decay, approximated by an exponential function^{10, 11}, is given by

$$P(t) = P_0 e^{-(t-t_d)/\theta} \quad 0 \leq t \leq \theta \quad (1)$$

For trinitrotoluene (TNT), the peak pressure (P_0) and the decay constant (θ) are given by

$$P_0 = 52.16 * 10^6 \left(\frac{W^{1/3}}{R} \right)^{1.13} \quad (2)$$

$$\theta = 92.5 * W^{1/3} \left[\frac{W^{1/3}}{R} \right]^{-0.22} \quad (3)$$

where $P(t)$ is the pressure at any instant of time t , P_0 the peak pressure of the shock front, θ the decay constant, t the time variable, W the charge weight, $t_d = (R-R_0)/c$ the time delay, R the stand-off distance, R_0 the shortest radial distance, and c the speed of sound in water.

Assuming the ship to be an infinite plate, the reflected pressure on the hull panels can be predicted reasonably accurately, based on the Taylor's plate theory¹² that uses linear acoustic approximation. The total pressure on the hull panel, considering fluid-structure interaction is given by

$$P_t = 2 * P(t) - [\rho c v(t) / \sin \phi] \quad (4)$$

where

$$v(t) = \frac{2 P_0}{\rho c} \frac{1}{z-1} \left\{ e^{(-t/z\theta)} - e^{(-t/\theta)} \right\} \quad (5)$$

$$z = \frac{m}{\rho c \theta} \quad (6)$$

$$\phi = \sin^{-1}(R_0/R) \quad (7)$$

Here, P_t is the total pressure on the plate at time t , ρ the fluid density, m the mass per unit area, z the characteristic mass ratio, $v(t)$ the hull panel velocity, and ϕ the angle of attack of the shock wave.

The above solution has been obtained by solving the 2-D wave equation for a case where plane wave is incident on a freely suspended infinite plate. The interface condition at plate-fluid boundary

is based on the velocity acquired by the plate, which is assumed to be rigid. Equation 4 has been widely used in the context of shock experiments, where the plate assembly is suspended.

3. FINITE ELEMENT ANALYSIS

3.1 Finite Element Formulation

The finite element analysis of the ship hull panels has been carried out using the CSA/GENSA (DYNA3D) nonlinear finite element code. The material nonlinearities are modelled by the Von-Mises yield criterion and its associated flow rule with a bilinear stress-strain law. The geometric nonlinearities are based on large deformation finite strain formulation. The finite element equations of motions for the assemblage of elements, derived based on the principle of virtual work, may be written in the form:

$$[M]\{\ddot{X}\} = \{P\} - \{F\} + \{H\} \quad (8)$$

where $[M]$ denotes the diagonal mass matrix, $\{P\}$ the sum of external and body force vectors, $\{F\}$ the stress divergence vector, and $\{H\}$ the hourglass resistance. The stress divergence vector and hourglass resistance vector⁹ are given by

$$\{F\} = \int_V B^T \sigma \, dv \quad (9)$$

$$\{H\} = -a_n \sum_{j=1}^4 h_{ij} r_{jk} \quad (i = 1, 3) \quad (10)$$

where

$$h_{ij} = \sum_k V_i^k r_{jk} \quad (11)$$

and

$$a_{,,} = Q_{ng} \rho v_e^{2/3} c / 4 \quad (12)$$

Here, B is the strain-displacement matrix (with t denoting the transpose), σ the stress vector, r_{jk} the hourglass base vector, h_{ij} the magnitude of hourglass mode, V_e the element volume, c the speed

of sound in the material, Q_{ng} a constant with value between 0.05 and 0.15 and V_i^k the nodal velocity of the k^{th} node in the i^{th} direction. A set of nonlinear equations given in Eqn (8) is solved using the central difference scheme.

3.2 Modelling of Hull Panels

The hull panels chosen for the analysis can be considered to be the shell portion between the two framings and the two stiffeners of any typical ship hull. The hull panels with a projected exposed area of $1.50 \times 0.60 \text{ m}^2$ have been modelled using four-noded Hughes-Liu shell element available in the CSA/GENSA code. Clamped edge condition has been assumed at the edges of the hull panel, and in view of symmetry, only one-fourth of the panel (consisting of 25×10 elements) need be considered for the analysis as shown in Fig. 1.

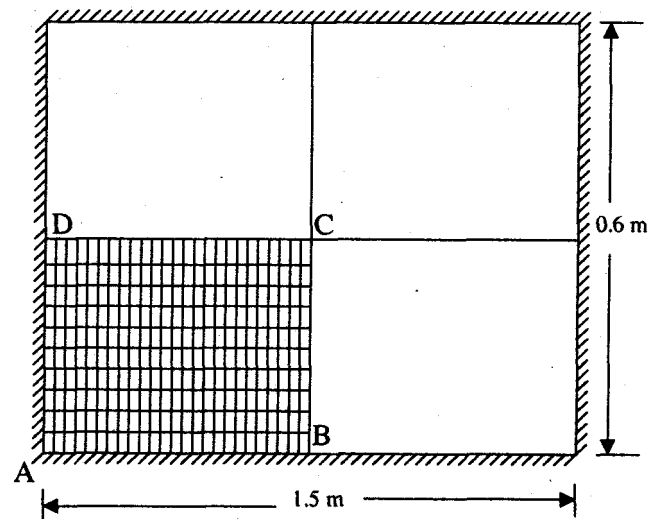


Figure 1. Finite element model of the hull panel

3.3 Estimation of Shock Loads

The explosion is assumed to be on the normal line passing through the centre of the hull panel, 5 m from the panel and the pressure loading has been calculated based on the Taylor's plate theory. The mass per unit area term (m) in the Taylor's equation considerably affects the loading history. For the present analysis, the mass value has been calculated assuming the ship's displacement to be

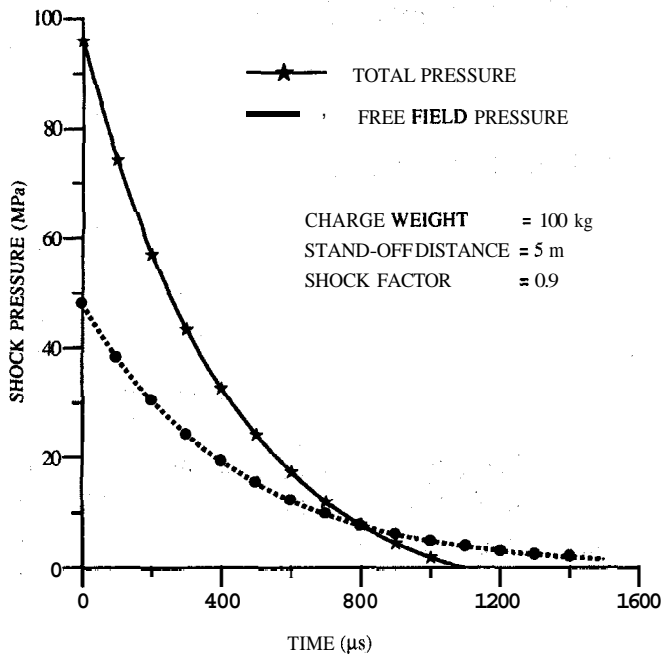


Figure 2. Typical pressure-time history

4500 ton. The area over which the pressure is more than 10 per cent of the maximum pressure is considered, as an approximation, for calculating the effective area exposed to shock. The mass term in the Taylor's plate theory [Eqn (6)] is calculated by dividing the ship's displacement by the effective area. Thus, the effective area is assumed to be $80 \times 9 \text{ m}^2$ and the corresponding mass per unit area is 6250 kg/m^2 .

The dimensions of the panels (a and b) are much smaller than the radial stand-off distance (R) of the charge location, ie, $(a/R)^2$ and $(b/R)^2 \ll 1$. Hence, the pressure whose time history given by Eqn (4), can be assumed to be uniform over the entire panel. A typical pressure-time history [both total and free field using Eqns (4) and (1)] at the centre of the panel corresponding to a 100 kg charge weight at 5 m stand-off distance is shown in Fig. 2, where the negative pressure is not included. The peak pressures estimated for various loading conditions on the hull panel are presented in Table 1.

3.4 Material Model

The constitutive model selected for the nonlinear analysis using the CSA/GENSA (DYNA3D)

Table 1. Shock pressure loading on the hull panel (stand-off distance = 5 m)

Charge weight (kg)	Shock factor ($0.45 \times W^{1/2}/R$) ($\text{kg}^{1/2}/\text{m}$)	Shock pressure (MPa)
1	0.090	16.9
2	0.127	22.0
3	0.156	25.6
5	0.201	31.0
10	0.285	40.3
25	0.450	56.9
50	0.636	73.9
75	0.779	86.0
100	0.900	95.9
125	1.000	104.0
150	1.100	112.0

explicit integration code is the elasto-plastic material model with isotropic hardening. The geometric nonlinear model is based on large deformation finite strain formulation. The other material properties used in the analysis are:

Elastic modulus (E)	= $2.1 \times 10^5 \text{ MPa}$
Poisson's ratio (ν)	= 0.3
Mass density (ρ)	= 7860.0 kg/m^3
Tangent modulus (E_t)	= 250.0 MPa
Static yield stress (σ_y)	= 400.0 MPa
Rupture strain (ϵ_{rup})	= 0.23

3.5 Strain Rate Effect

To include the effect of strain rate in the finite element analysis, the elasto-plastic analysis has been first carried out ignoring this effect, ie, the static yield stress has been employed in the analysis. Subsequently, the strain rate has been calculated from the maximum effective plastic strain curves [Eqn(14)] obtained from the analysis. The average strain rate is calculated for time duration from the start to the point, where the strain is nearly constant from the effective plastic strain time history. The strain rate effect has been included using this average strain rate value in the Cowper-Symonds relation¹³ to compute the dynamic yield stress (σ_{dy}), ie

$$\sigma_{dy} = \sigma_y \left(1 + \left| \frac{\dot{\epsilon}}{D} \right|^{\frac{1}{n}} \right) \quad (13)$$

where σ_y is the static yield stress, and D and n are the other material parameters. In the present calculations, $D=401$ s and $n=5$, being the commonly accepted values for steel, have been used.

3.6 Failure Criteria for Tensile Tearing

Finite element modelling of the concentrated plastic hinge near the clamped boundary would entail unduly large meshes to predict the response accurately. In view of this, it is assumed that tearing will be initiated if the effective plastic strain at the edge (ϵ_{eff}) (based on the simpler finite element model) is greater than the rupture strain. The effective plastic strain⁹ at the edge of the plate is given by

$$\epsilon_{eff} = \int_0^t \left(\frac{2}{3} \dot{\epsilon}_{ij}^p \dot{\epsilon}_{ij}^p \right)^{1/2} dt \quad (14)$$

and the plastic strain rate ($\dot{\epsilon}_{ij}^p$), which is a function of total strain rate ($\dot{\epsilon}_{ij}$) and elastic strain rate ($\dot{\epsilon}_{ij}^e$), is given by

$$\dot{\epsilon}_{ij}^p = \dot{\epsilon}_{ij} - \dot{\epsilon}_{ij}^e \quad (15)$$

Olson², et al. proposed a total strain criterion, according to which tensile tearing is said to be initiated if the total strain (bending + membrane) exceeds rupture strain.

3.7 Nondimensional Plot

Postulating a deformed shape of the hull panel with average slopes of $2\delta/a$ and $2\delta/b$ (δ being the mid-point deformation) along the two central lines of the panel and applying a stress of σ_0 , uniformly along the edges, the total load intensity (F) on the panel may be written as

$$F \propto \sigma_0 \frac{4\delta h}{a^2} \left(1 + \frac{a^2}{b^2} \right) \quad (16)$$

where a and b are the side dimensions of the hull panel and h its thickness. In view of the Eqn (16), a nondimensional load F_n and nondimensional displacement⁷ β are defined as

$$F_n = \frac{P_{max}}{\sigma_0} \quad (17)$$

$$\beta = \frac{\delta h}{a^2} \left(1 + \frac{a^2}{b^2} \right) \quad (18)$$

where P_{max} is the maximum peak shock overpressure [obtained from Eqn (4)] on the plate. For plotting, F_n has been defined in two ways, one with $\sigma_0 = \sigma_{dy}$, the dynamic yield stress and the other with $\sigma_0 = \sigma_y$, the static yield stress.

4. RESULTS & DISCUSSION

The mass per unit area of the plate in the Taylor's plate equation considerably affects the total pressure experienced by the plate as a result of fluid-structure interaction. In view of this, the interaction pressure loading on the hull panel was estimated for the three different mass factors of 0.5, 1.0, and 1.5. The mass factor is defined as the ratio of mass in the Taylor's plate equation [m in Eqn(6)] to the displacement of the ship. The variation of pressure for the three different mass conditions, for a particular charge weight of 100 kg at 5 m stand-off distance is shown in Fig. 3. Even though the initial total pressure is the same for all the mass conditions, the pressure wrt time varies considerably, for the three cases. The duration of the pulse increases with 'increase in mass term, indicating that the heavier ships experience pressure loading for a longer duration. This means that the explosion energy is distributed over a longer time for heavier ships, which would result in reduced damage.

Since the mass value required in the calculation of interaction pressure could not be accurately estimated, sensitivity analysis on the response of the hull panel (flat) for the three different mass conditions for a charge weight of 100 kg were

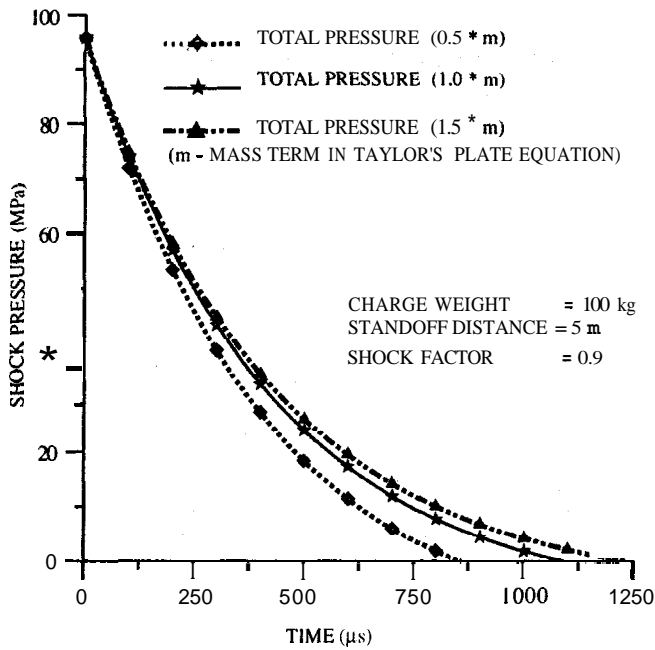


Figure 3. Comparison of pressure-time histories for various mass ratios ($m = 6250 \text{ kg/m}^2$).

carried out. The corresponding response parameters were found to vary considerably, as shown in Table 2. The deformation has been found to increase with reduction in mass. In the present case, the deformation reduces by about 36 per cent, when the mass term is increased by 50 per cent. In the same way, a reduction in mass ratio by 50 per cent increased the response by 30 per cent. This indicates that for the lighter ships, the local damage would be more, whereas the heavier ships would suffer lesser damage, for a particular charge configuration.

The other loading configurations were analysed only for a mass factor of 1. Typical displacement-time histories at the centre of the panel with and

Table 2. Response of fiat hull panel for various mass conditions (charge weight $\approx 100 \text{ kg}$; stand-off distance = 5 m; shock factor = $0.9 \text{ kg}^{1/2}/\text{m}$)

Mass factor *	Deformation (m)	Strain rate (1/s)	Dynamic yield (MPa)
0.5	0.220	527.7	1070
1.0	0.172	476.0	1054
1.5	0.110	319.8	1006

* Mass factor = Mass value in the Taylor's plate equation / displacement of the ship.

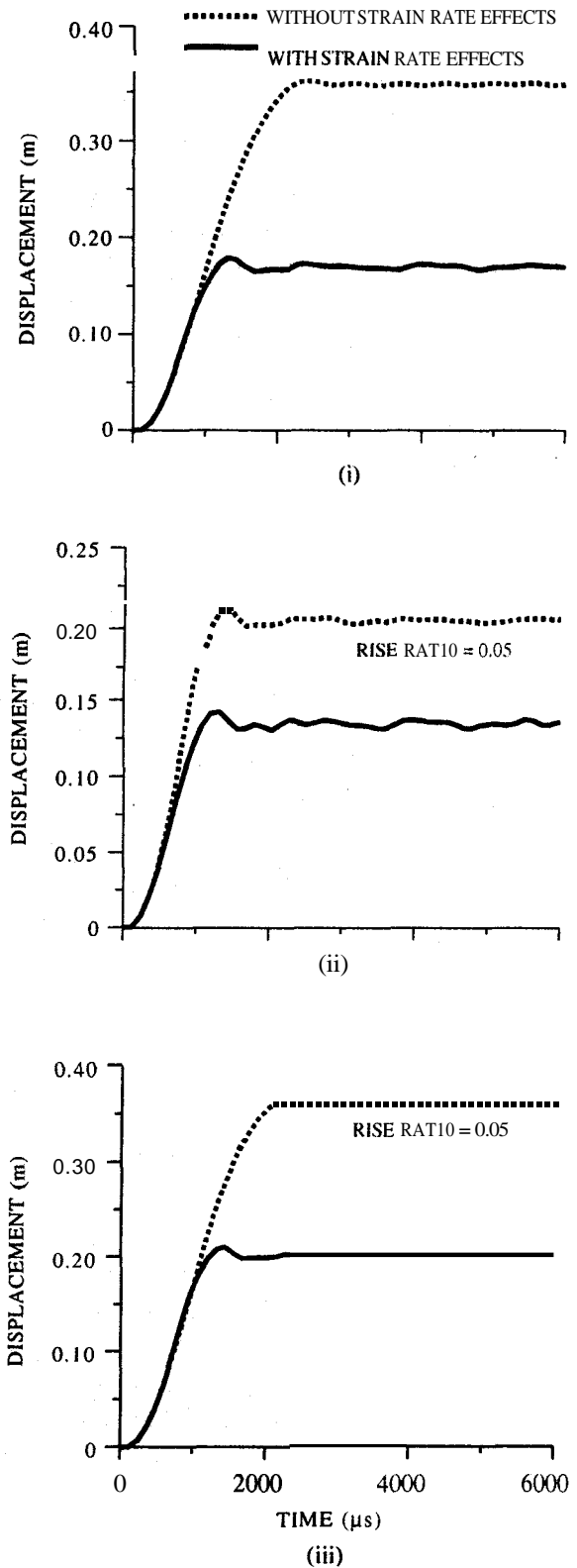


Figure 4(a). Displacement-time history at the centre for various hull panels (point C in Fig. 1) : (i) flat panel (ii) concave panel, and (iii) convex panel.

without strain rate effects for all the three types of panels are shown in Fig. 4 (a). The displacement-time history is found to increase monotonically till the maximum, and oscillate thereafter. The deformation is computed from the total displacement by subtracting the elastic deformation, which however seems to be very small. The displacement-time history and the time of occurrence of peak displacement are considerably affected because of strain rate effects, as has been noted for thinner test panels^{6,8}.

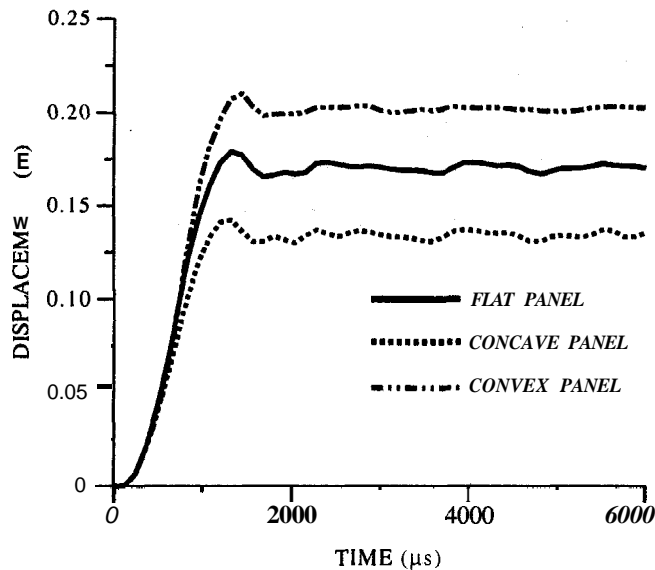


Figure 4(b). Comparison of displacement-time histories at the centre for the hull panel (point C in Fig. 1).

A comparison of the displacement-time histories considering strain rate effects for flat and curved panels are shown in Fig. 4(b). It is observed that the convex cylindrical panels experience more plastic deformation than the flat panels because of snap-through-behaviour. The concave cylindrical shell panels suffer a lesser permanent deformation than the flat panels because of membrane resistance offered by the initial curvature.

The shock factor ($SF = 0.45 \cdot W^{1/2}/R$; W the charge weight, R the stand-off distance) versus permanent deformation for all the three types of panels is plotted in Fig. 5. The permanent deformation is found to increase for all the three panels with increase in shock factors, with the

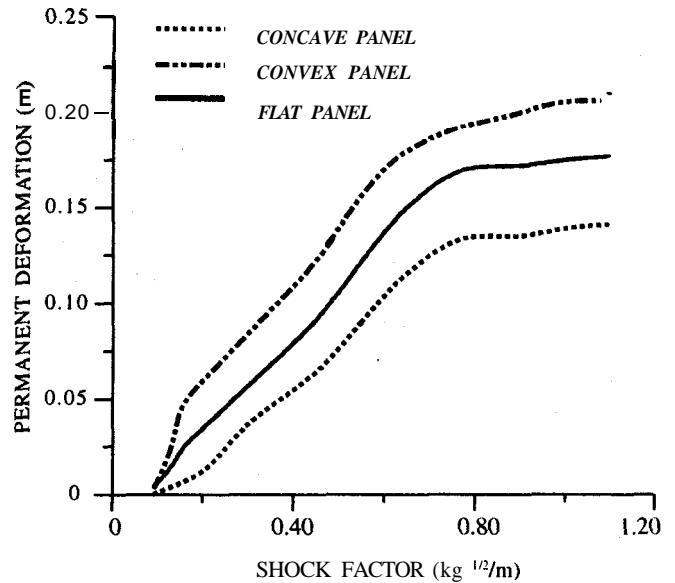
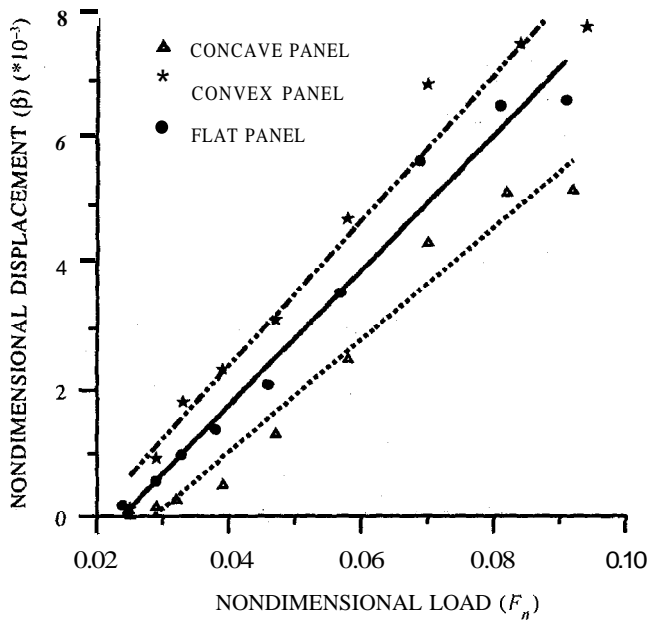


Figure 5. Shock factor versus permanent deformation for the hull panels (point C in Fig. 1).

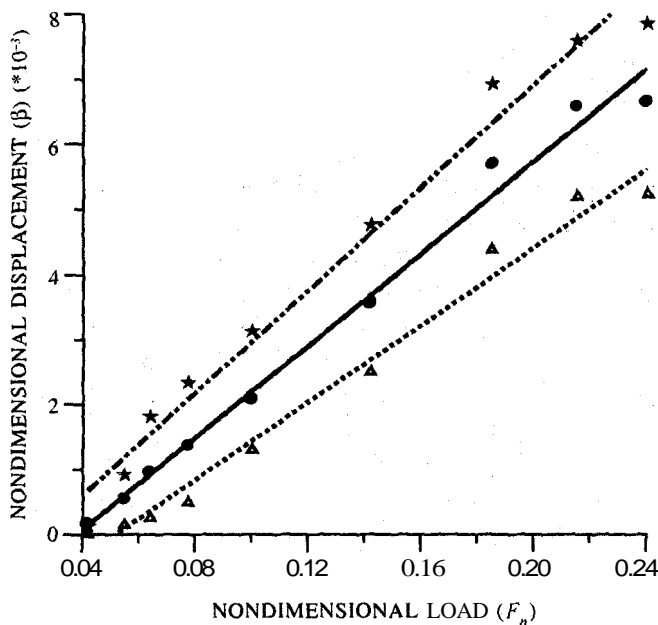
concave panels offering better resistance to shock loads.

A plot of F_n versus β [Eqns (17) and (18)] incorporating both static yield stress (σ_y) and dynamic yield stress (σ_d) for the various hull panels are shown in Fig. 6 along with the best-fit line. The qualitative difference between the plots in Figs 6(a) and 6(b) can be ascribed to the rate sensitivity of the plate material, which plays an important role in response prediction. A major difficulty with the dynamic yield stress-based plot is that it needs the average strain rate value to predict the dynamic yield stress, which has to be obtained from a nonlinear finite element analysis. The plot in Fig. 6(b) should be of particular interest to the designers.

The variation of effective plastic strain wrt shock factor is plotted in Fig. 7 for all the three types of hull panels considered in the analysis. The effective plastic strain values are found to be higher for the flat panels compared to the curved panels, for a particular shock load. It has been observed from Fig. 7 that the effective strain value exceeds the rupture strain value for shock factors $0.32 \text{ kg}^{1/2}/\text{m}$, $0.34 \text{ kg}^{1/2}/\text{m}$, and $0.4 \text{ kg}^{1/2}/\text{m}$ for the flat, the concave, and the convex



(a)



(b)

Figure 6. Plot of nondimensional load versus displacement for hull panels (finite element model):
(a) $F_n = P_{\max}/\sigma_{dy}$ and (b) $F_n = P_{\max}/\sigma_y$

panels respectively, indicating that the tearing was initiated at the above shock factors. Similarly, the variation of total strain² wrt the shock factor is plotted in Fig. 8. For shock factors of **0.34 kg^{1/2}/m**, **0.36 kg^{1/2}/m** and **0.44 kg^{1/2}/m**, the total strain value exceeds the rupture strain value,

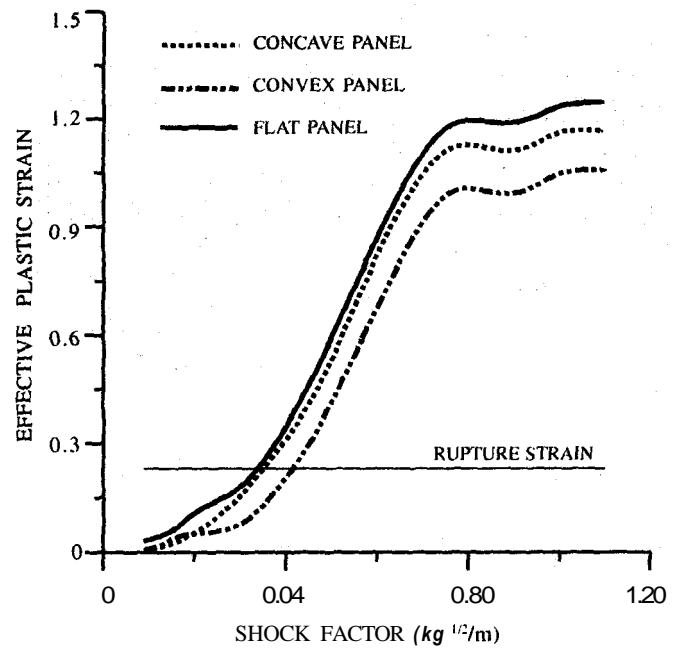


Figure 7. Shock factor versus effective plastic strain (point B in Fig. 1).

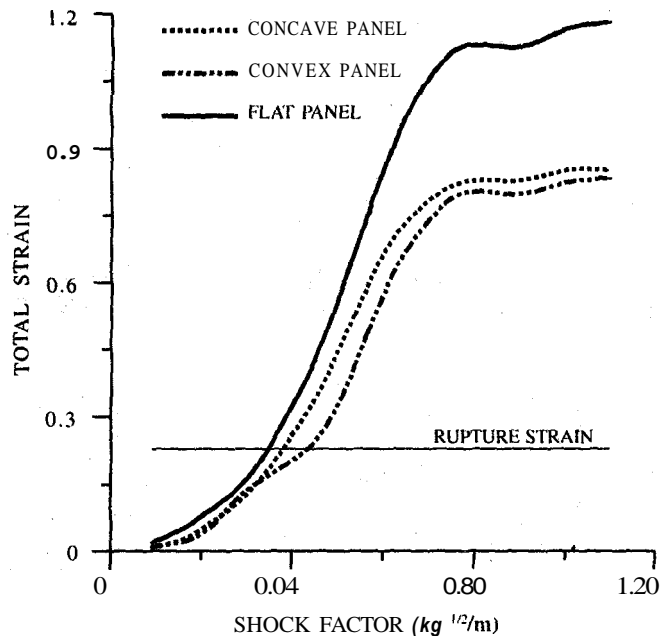


Figure 8. Shock factor versus total strain (point B in Fig. 1)

indicating tearing at the edges for flat, concave, and convex panels, respectively. Both the strain criteria (effective and total) indicate that the flat panels suffer tearing for a specific shock load compared to the other panels, with the convex panels offering more resistance before rupture.

5. CONCLUSIONS

The deformation of typical hull panels under shock loading has been studied employing the nonlinear finite element analysis. The pressure loading on the hull panel due to underwater explosion has been estimated based on plane wave approximation. The strain rate effects have been included using the Cowper-Symonds relation.

The concave hull panels suffer lesser deformation than the flat and the convex panels when subjected to underwater explosion of the same intensity. This is because the action of the shell membrane and the action of the nonlinear membrane reinforce each other in the concave panels. On the other hand, convex panels suffer dynamic snap-through-behaviour. Despite larger permanent deformation, the results indicate that convex hull panels can withstand larger shock loads before reaching the tensile-tearing failure mode compared to the other panels. A linear-fit between the loads and the permanent deformation should be explored to formulate design charts employing finite element analysis.

ACKNOWLEDGEMENT

The authors gratefully acknowledge Rear Adm S. Mohapatra, Director, Naval Science & Technological Laboratory (NSTL), Visakhapatnam, for permission to publish this work.

REFERENCES

1. Menkes, S.B. & Opat, H.J. Tearing and shear failure in explosively loaded clamped beams. *Explosion Mechanics*, 1973, **13**, 480-86.
2. Olson, M.D.; Nurick, G.N. & Fagnan, J.R. Deformation and rupture of blast-loaded square plates—predictions and experiments. *Int. J. Impact Engg.*, 1993, **13**, 279-91.
3. Nurick, G.N.; Olson, M.D.; Fagnan, J.R. & Levin, A. Deformation and tearing of blast-loaded stiffened square plates. *Int. J. Impact Engg.*, 1995, **16**, 273-91.
4. Nurick, G.N. & Shave, G.C. Deformation and tearing of thin square plates subjected to impulsive loading. *Int. J. Impact Engg.*, 1996, **18**, 99-116.
5. Ahmed, J.; Wong, K. & Porter, J. Nonlinear dynamic analysis assessment of explosively-loaded submarine hull panels. *Shock Vib. Bull.*, 1990, **60**(1), 139-71.
6. Ramajeyathilagam, K.; Vendhan, C. P. & Bhujanga Rao, V. Nonlinear transient dynamic response of rectangular plates under shock loading. *Int. J. Impact Engg.*, 2000, **24**, 999-1015.
7. Ramajeyathilagam, K. Experimental and numerical investigations on the response of structural elements to underwater explosion. Indian Institute of Technology Madras, Chennai, 2000. **PhD Thesis**.
8. Ramajeyathilagam, K.; Vendhan, C.P. & Bhujanga Rao, V. Experimental and numerical investigations on deformation of cylindrical shell panels to underwater explosion. *J. Shock Vib.*, 2001, **8**, 253-70.
9. CSA/GENSA user manual. CSA Research Corporation, California, USA, 1996.
10. Cole, R.H. Underwater explosions. Dover Publications Inc, New York, USA, 1948.
11. Keil, A.H. The response of ships to underwater explosion, *Trans. Soc. Naval Architects Marine Engg.*, 1961, **69**, 366-10.
12. Taylor, G.I. The pressure and impulse of submarine explosion waves on plates. Compendium of Underwater Explosion Research, ONR, 1950, **1**, 1155-174.
13. Jones, N. Structural impact. Cambridge University Press, Cambridge, UK, 1989.

Contributors

Dr K Ramajeyathilagam obtained his **MTech** and **PhD** (Ocean Engg) both from the **Indian Institute of Technology Madras, Chennai**. Presently, he is working as Scientist at the Naval Science & Technological Laboratory (NSTL), Visakhapatnam. His areas of work include: Underwater **shock, shock response** of ships, submarines, and naval equipment, and finite element analysis. He has received a commendation certificate from the Scientific Adviser to **Raksha Mantri** for his **research** work in the area of response of ships and submarines subjected to underwater **explosion**.

Prof CP Vendhan obtained his **PhD** (Civil Engg) from the Indian Institute of Technology (IIT), Kanpur and postdoctoral research from the University of **Massachusetts, USA**. He is presently working as Professor at the IIT Madras, **Chennai**, in the Dept of Ocean Engineering. His areas of research include: **Fluid-structure** interaction, dynamics of floating bodies and offshore structures. He has guided a number of **PhD students** and has about 50 research papers published in the international journals.